Invited paper

Application of multiresolution analysis to the modeling of microwave and optical structures

C. D. SARRIS[1], L. P. B. KATEHI[1] AND J. F. HARVEY[2]
[1]*Radiation Laboratory, Department of Electrical Engineering and Computer Science, University of Michigan, Ann Arbor, MI, 48109-2122, USA (E-mail: ksarris@umich.edu)*
[2]*United States Army Research Office, Research Triangle Park, NC 27709, USA*

Abstract. A review of wavelet based techniques for the modeling of electromagnetic and optical structures is provided in this paper. Fundamental theoretical aspects of Multiresolution Analysis are mentioned along with mathematical properties of wavelet bases that lead to the construction of highly efficient numerical schemes and fast algorithms. Applications of such schemes in the field of time and frequency domain analysis of electromagnetic geometries are shown and the recently developed Multiresolution Time Domain technique is extensively presented. The analysis and evaluation of wavelet based techniques indicates their potential to provide fast and accurate solutions, thus broadening the limits of existing electromagnetic solvers.

Key words: frequency domain, multiresolution analysis, time domain, wavelets

1. Introduction

For more than one decade, wavelet theory has been a field of intensive multidisciplinary research for mathematicians, physicists and engineers. A strong motivation for this activity has been provided by the property of many wavelet bases to exhibit time and frequency localization (Daubechies 1992), thus broadening the limits of the traditional Fourier analysis of functions and distributions (Meyer 1992). Due to this property, the use of wavelets has become an efficient tool in the study of a variety of applications in different areas of science and engineering.

Among the areas where wavelet based techniques have shown significant promise is the solution of boundary value problems, encountered in the process of numerical modeling of important physical phenomena that contain singularities or sharp transitions. Examples of the latter are the formation of shock waves in fluid dynamics and beam focusing in nonlinear optics (Bacry *et al.* 1992). Furthermore, state of the art microwave geometries typically contain localized fine details, whose accurate modeling requires a high order mesh refinement. In such cases, the cost of modeling either a spatially isolated detail or a singularity may adversely affect the overall computational burden of a simulation, unless an adaptive method is employed. Wavelets and the concept of Multiresolution Analysis (MRA)

provide a natural framework for the implementation of highly efficient adaptive numerical schemes that overcome the well known difficulties attached to multigrid techniques (Berger and Oliger 1984).

According to MRA, an approximation of a function at a certain resolution can be considered as an approximation of this function at a coarse resolution (generated by the so called *scaling* basis functions), successively refined by wavelet functions. Hence, the local regularity of a certain function is merely reflected on the magnitude of its wavelet expansion coefficients. The latter can be either retained in computer memory or thresholded to zero (according to their relative magnitude), a procedure that adaptively tailors the computer time and memory demands of the wavelet based algorithm to the problem at hand.

Another aspect of MRA that leads to the construction of fast algorithms is the Fast Wavelet Transform (Mallat 1989), that allows for the wavelet decomposition of a given function in a recursive manner at the optimal cost of $\mathcal{O}(N)$ operations.

The combination of these attractive features of wavelet based numerical analysis has led to the development of both time domain and frequency domain techniques with significantly improved properties compared to their conventional counterparts. This paper provides a selective review of such techniques, emphasizing their application to the solution of electromagnetic and optical problems.

2. Overview of multiresolution analysis

This section presents a brief overview of the mathematical properties of wavelets and multiresolution analysis without delving into details that can be found in relevant texts such as (Daubechies 1992; Meyer 1992). Also, this analysis is restricted to orthonormal wavelet bases, although non-orthogonal wavelet systems (for example, *biorthogonal* wavelets (Cohen *et al.* 1992)) have been employed in a number of applications (Aidam and Russer 1998).

2.1. MULTIRESOLUTION APPROXIMATIONS

Wavelet bases are a mathematical tool for hierarchical decomposition of functions in an orthogonal expansion, according to the general scheme:

$$f(\xi) = \sum_k c_k \phi(\xi - k) + \sum_j \sum_k d_{j,k} \psi(2^j \xi - k) \tag{1}$$

where f is assumed to belong to $L^2(\mathbb{R})$[1]. In Equation (1), the first sum represents the projection of $f(\xi)$ onto a subspace V_0, that corresponds to an

---

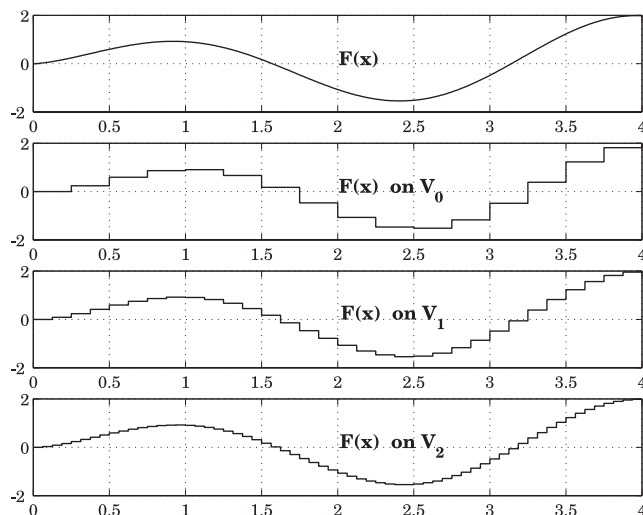[1] Hilbert space of square integrable functions.

Fig. 1. Projections of a function f on three approximation spaces V_0, V_1, V_2.

approximation of f at a 'coarse' level of resolution. The basis of V_0 is generated by orthogonal translations of $\phi(\xi)$ which is called the *scaling* function. The resolution of V_0 is successively refined by the second sum which consists of projections of f onto the subspaces W_j, each one being spanned by a *wavelet* basis $\{\psi(2^j\xi - k)\}$. The function $\psi(\xi)$ is called the *mother wavelet*, since all other wavelet basis functions $\psi_{j,k}$ are simply produced by dilations (for adjustement of resolution) and translations of ψ. It is noted that a basic property of the subspaces V_0, W_0 is:

$$V_0 \oplus W_0 = V_1 \tag{2}$$

where V_1 corresponds to a level of resolution twice that of V_0. This means that scaling and zero wavelet functions form a basis of orthogonal functions that spans V_1. The notion of a projection of f onto approximation spaces at successive levels of resolution is explained in Fig. 1.

Recursively,

$$V_0 \oplus W_0 \oplus W_1 \cdots \oplus W_{k-1} = V_k \tag{3}$$

In other words, adding one wavelet level, is equivalent to improving the resolution of an approximation, like the one in Equation (1), by a factor of two[2]. Hence, any desired resolution of approximation can be achieved by adding an appropriate number of wavelet levels.

---

[2] Dyadic multiresolution analyses are considered here. In general, modifying the dilation factor for the generation of the wavelet basis from the mother wavelet can yield other types of MRA.

The advantage of this approach lies in the dependence of the magnitude of wavelet coefficients on the local regularity of f. In particular, wavelet coefficients assume large values near discontinuities or singularities. Therefore, once a numerical analysis of a problem is performed by expanding the unknown function in a wavelet basis, high order wavelet coefficients which are located away from discontinuities or singularities, typically assume insignificant values that can be thresholded to zero. By this procedure, an adaptive, temporally moving mesh is implemented.

2.2. WAVELET BASES

The simplest (and oldest) orthogonal wavelet system is the *Haar* basis (Haar 1910). Its study is useful from a theoretical point of view because it offers an intuitive understanding of many multiresolution properties. Furthermore, due to its simplicity, this basis is widely employed in a series of applications, hence its study is also practically interesting.

The Haar scaling function is defined as a pulse of unit length:

$$\phi(\xi) = \begin{cases} 1, & 0 \leq \xi < 1 \\ 0, & \text{otherwise} \end{cases} \tag{4}$$

and the scaling function basis is produced by orthogonal translations of the latter:

$$\phi_k(\xi) = \phi(\xi - k) \tag{5}$$

The Haar mother wavelet function is defined as:

$$\psi(\xi) = \begin{cases} 1, & 0 \leq \xi < 1/2 \\ -1, & 1/2 \leq \xi < 1 \\ 0, & \text{otherwise} \end{cases} \tag{6}$$

and the basis is now produced by both translations and dilations, as shown in the definition:

$$\psi_{j,k}(\xi) = 2^{j/2}\psi(2^j\xi - k) \tag{7}$$

In all these definitions ξ is a normalized, dimensionless variable. For example, if ϕ or ψ functions represent a variation along the x-direction of a computational mesh with a cell size Δx, then simply: $\xi = x/\Delta x$. The Haar scaling and mother wavelet functions are depicted in Fig. 2, and the mechanism, in which multiresolution analysis is brought about by employing this basis (in the sense of Equation (3)), is qualitatively explained in Fig. 3.
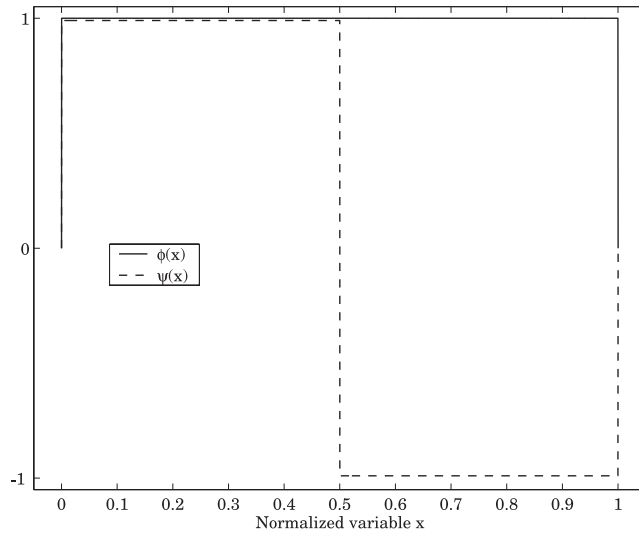
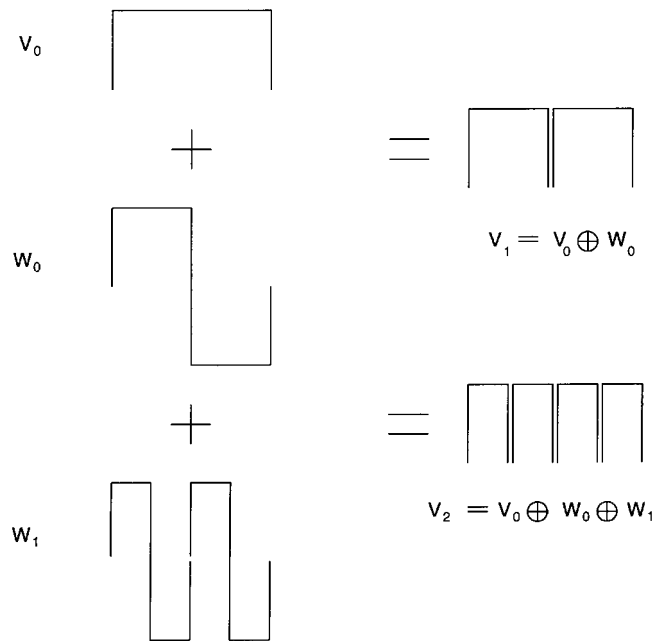Fig. 2. Haar scaling and mother wavelet functions.

Fig. 3. Demonstration of the multiresolution principle.

The Haar basis has an excellent localization in space (or time) domain and poor localization in the corresponding Fourier domain, as shown in Fig. 4. Therefore, the Haar basis does not share the typical wavelet property of
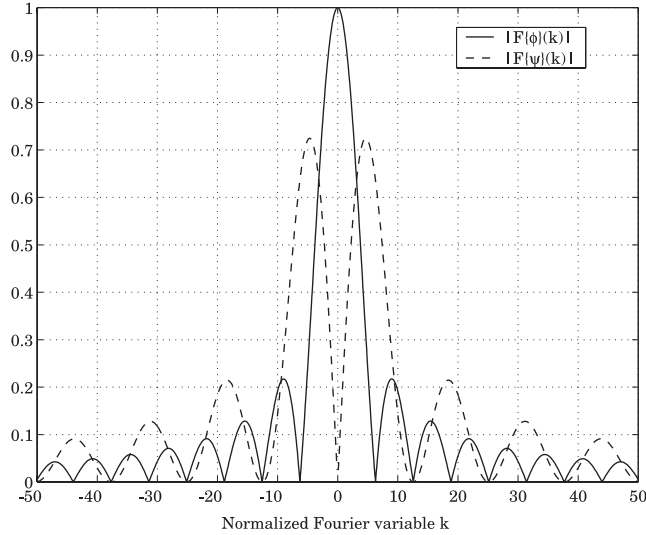
Fig. 4. Haar scaling and mother wavelet functions in the Fourier domain.

combining good localization in both domains (within the limits of the un-
certainty principle (Mallat 1998)). Throughout this work, the following
definition has been adopted for the Fourier transform:

$$\mathscr{F}\{f\}(k) = \int_{-\infty}^{+\infty} f(\xi)e^{jk\xi}\,\mathrm{d}\xi \tag{8}$$

A basis that has also been used in applications, is the cubic spline Battle–
Lemarie basis (Battle 1987). The Battle–Lemarie scaling and mother wavelet
(Fig. 5) are entire domain functions and therefore schemes that are developed
in this basis have to be truncated with respect to space. However, Battle–
Lemarie scaling and wavelets have an excellent localization both in space and
Fourier domains (Fig. 6), a feature that permits an *a priori* estimate of the
necessary levels of resolution for correct field modeling.

   Figs. 4 and 6 also provide an intuitive explanation of the successive ap-
proximation procedure that is connected to multiresolution analysis. Evi-
dently, the scaling function has the Fourier domain pattern of a *low-pass
filter*, while the mother wavelet is by the same token a *band-pass filter*. Hence,
scaling functions alone provide a description of 'low frequency' character-
istics of a signal, while the addition of wavelets enhances the capability of a
scheme to describe the high frequency content of a signal. This argument also
explains the adaptivity property of wavelet based numerical schemes:
Wavelet coefficients correspond to high frequency signal variations, in the
absence of which, the value of these coefficients decays to insignificant levels.
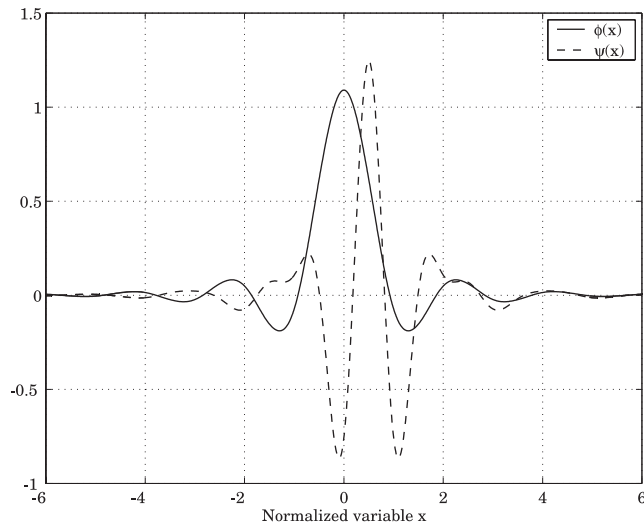
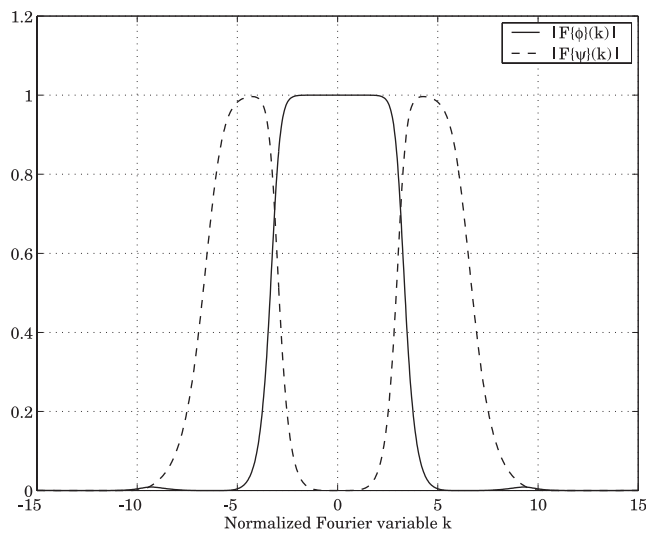Fig. 5. Battle–Lemarie scaling and mother wavelet functions.

Fig. 6. Battle–Lemarie scaling and mother wavelet functions in the Fourier domain.

3. Wavelet based time domain schemes

The concepts of wavelet based numerical analysis have been successfully applied to the field of time domain analysis of microwave circuits, with the introduction of the Multiresolution Time Domain (MRTD) technique (Krumpholz and Katehi 1996). In fact, several types of MRTD schemes can be derived, depending on the wavelet basis that is employed for the discreti-

zation of Maxwell's equations. Analysis and study of MRTD has demonstrated its significantly better performance, in terms of memory and execution time requirements, than the Finite Difference Time Domain (FDTD) technique (Taflove 1995). The latter has recently become very popular due both to its versatility and simplicity and the advancement of computer performance that can nowadays reasonably meet the FDTD computational demands, which for medium to large scale problems can become extremely high. In this section, the application of the Method of Moments (MoM) for the derivation of Time Domain schemes is first demonstrated for a simple, pulse basis. By extending this method, two MRTD schemes are then derived and analyzed.

3.1. DERIVATION OF TIME DOMAIN SCHEMES BY THE METHOD OF MOMENTS

The formulation of the MRTD technique is based on the observation in (Krumpholz *et al.* 1995) that the FDTD scheme can be rigorously derived by applying the MoM (Harrington 1968). This concept is here explained by considering the simple example of the one dimensional, one way wave equation (Krumpholz and Katehi 1997):

$$\frac{\partial E(z,t)}{\partial z} = \frac{1}{c}\frac{\partial E(z,t)}{\partial t} \tag{9}$$

For the numerical solution of this equation, a discrete space-time mesh is introduced and the values of the electric field $E(m\Delta z, k\Delta t) = {}_kE_m$ are sought by marching in time. The FDTD scheme for this equation is derived by approximating the partial derivatives of each side of the equation at a space-time mesh point $(m\Delta z, k\Delta t)$, by centered differencing (Strikwerda 1989):

$$\frac{\partial E(m\Delta z, k\Delta t)}{\partial z} = \frac{E((m+1)\Delta z, k\Delta t) - E((m-1)\Delta z, k\Delta t)}{2\Delta z} + O(\Delta z^2)$$
$$\approx \frac{{}_kE_{m+1} - {}_kE_{m-1}}{2\Delta z} \tag{10}$$

$$\frac{\partial E(m\Delta z, k\Delta t)}{\partial t} = \frac{E(m\Delta z, (k+1)\Delta t) - E(m\Delta z, (k-1)\Delta t)}{2\Delta t} + O(\Delta t^2)$$
$$\approx \frac{{}_{k+1}E_m - {}_{k-1}E_m}{2\Delta t} \tag{11}$$

Simple algebraic manipulation leads to a second-order accurate approximation of (9):

$$_{k+1}E_m = {}_{k-1}E_m + \frac{c\Delta t}{\Delta z}\left({}_kE_{m+1} - {}_kE_{m-1}\right) \tag{12}$$
$$= {}_{k-1}E_m + s\left({}_kE_{m+1} - {}_kE_{m-1}\right) \tag{13}$$

where $s = (c\Delta t)/\Delta z$ is the CFL (Courant–Friedrichs–Levy) number (Strik-werda 1989). For this scheme to be stable, the CFL number has to be less than unity. Alternatively, for the discretization of (9) via the MoM, the electric field $E(z, t)$ is expanded in pulse basis functions (or equivalently Haar scaling functions) $\{h_n(z)\}, \{h_n(t)\}$ in space and time:

$$E(z, t) = \sum_{k,m} {}_k E_m h_m(z) h_k(t) \tag{14}$$

with

$$h_n(x) = \begin{cases} 1, & n\Delta x \leqslant x < (n+1)\Delta x \\ 0, & \text{otherwise} \end{cases} \tag{15}$$

Substituting into (9), yields:

$$\sum_{k,m} {}_k E_m \frac{\mathrm{d}h_m(z)}{\mathrm{d}z} h_k(t) = \frac{1}{c} \sum_{k,m} {}_k E_m h_m(z) \frac{\mathrm{d}h_k(t)}{\mathrm{d}t} \tag{16}$$

Then, (16) is sampled in space and time using the complex conjugate of the basis functions themselves as testing functions (Galerkin method). To carry out the testing procedure, the following integrals are employed:

$$\int_{-\infty}^{+\infty} h_n(x) \frac{\mathrm{d}h_{n'}(x)}{\mathrm{d}x} \mathrm{d}x = \frac{1}{2}\left(\delta_{n',n+1} - \delta_{n',n-1}\right) \tag{17}$$

$$\int_{-\infty}^{+\infty} h_n(x) h_{n'}(x) \mathrm{d}x = \delta_{n',n}\Delta x \tag{18}$$

where $\delta_{n',n}$ is Kronecker's delta:

$$\delta_{n',n} = \begin{cases} 1, & \text{if } n' = n \\ 0, & \text{if } n' \neq n \end{cases}$$

Hence, testing the left handside of (16):

$$\int_{-\infty}^{+\infty} \int_{-\infty}^{+\infty} \mathrm{d}z \, \mathrm{d}t \, h_m(z) \, h_k(t) \frac{\partial E(z, t)}{\partial z} = \sum_{k',m'} \left(\delta_{m',m+1} - \delta_{m',m-1}\right) \delta_{k',k} \; {}_{k'} E_{m'} \frac{\Delta t}{2}$$

$$= \left({}_k E_{m+1} - {}_k E_{m-1}\right) \frac{\Delta t}{2} \tag{19}$$

while testing the right handside of (16):

$$\int_{-\infty}^{+\infty}\int_{-\infty}^{+\infty} \mathrm{d}z\,\mathrm{d}t\, h_m(z)h_k(t)\frac{1}{c}\frac{\partial E(z,t)}{\partial t} = \sum_{k',m'}\delta_{m',m}\left(\delta_{k',k+1}-\delta_{k',k-1}\right){}_{k'}E_{m'}\frac{\Delta z}{2c}$$

$$= \left({}_{k+1}E_m - {}_{k-1}E_m\right)\frac{\Delta z}{2c} \tag{20}$$

It is thus easily concluded that Equation (13) is again derived and therefore the two methods for approximating (9) in a discrete space are found to be equivalent.

In a similar manner, expanding the electric and magnetic fields in scaling and wavelet functions and applying the MoM for the discretization of Maxwell's equations (as indicated in the previous section), the MRTD scheme is derived. In this case, the field expansion in (14) writes:

$$E(z,t) = \sum_{k,m}{}_k E_m^{\phi}\phi_m(z)h_k(t) + \sum_{k,m}\sum_{r=0}^{R_{\max}}\sum_{p=0}^{2^r-1}{}_k E_m^{\psi_{r,p}}\psi_{m,p}^r(z)h_k(t) \tag{21}$$

where $R_{\max}$ is the maximum wavelet order that has been introduced. Also,

$$\phi_m(z) = \phi\left(\frac{z}{\Delta z} - m\right) \tag{22}$$

is a scaling basis produced by a scaling function ϕ and

$$\psi_{m,p}^r(z) = 2^{r/2}\psi\left(2^r\left(\frac{z}{\Delta z} - m\right) - p\right) \tag{23}$$

with $p = 0, 1, \ldots, 2^r - 1$. Hence, a slightly modified definition with respect to (1) is used for the wavelet basis here, in order to keep a correspondence between the cell index m of the scaling and the wavelet functions. The modified finite difference equations for the MRTD approximation of (9) are now dependent on the form that the following integrals assume in a given wavelet basis:

$$
\begin{aligned}
I_{n,n'}^{\phi,\phi} &= \int_{-\infty}^{+\infty}\phi_n(z)\frac{\mathrm{d}\phi_{n'}(z)}{\mathrm{d}z}\,\mathrm{d}z \\
I_{n,n'}^{\phi,\psi} &= \int_{-\infty}^{+\infty}\phi_n(z)\frac{\mathrm{d}\psi_{n',\,p}^r(z)}{\mathrm{d}z}\,\mathrm{d}z \\
I_{n,n'}^{\psi,\phi} &= \int_{-\infty}^{+\infty}\psi_{n,\,p}^r(z)\frac{\mathrm{d}\phi_{n'}(z)}{\mathrm{d}z}\,\mathrm{d}z \\
I_{n,n'}^{\psi,\psi} &= \int_{-\infty}^{+\infty}\psi_{n,\,p}^r(z)\frac{\mathrm{d}\psi_{n',\,p'}^{r'}(z)}{\mathrm{d}z}\,\mathrm{d}z.
\end{aligned}
\tag{24}
$$

3.2. BATTLE–LEMARIE MRTD SCHEMES

As an example, for the Battle–Lemarie scaling function (Krumpholz and Katehi 1997):

$$\int_{-\infty}^{+\infty} \phi_n(z) \frac{\mathrm{d}\phi_{n'}(z)}{\mathrm{d}z} \mathrm{d}z \approx \sum_{i=-15}^{i=15} a(i)\delta_{n',n+i} \tag{25}$$

where the coefficients $a(i)$ are numerically computed in the spectral domain, utilizing the spectral form of the Battle–Lemarie scaling function:

$$\mathscr{F}\{\phi\}(k) = \left(1 - \frac{4}{3}\sin^2\left(\frac{k}{2}\right) + \frac{2}{5}\sin^4\left(\frac{k}{2}\right) - \frac{4}{315}\sin^6\left(\frac{k}{2}\right)\right)^{-\frac{1}{2}}\left(\frac{\sin\left(\frac{k}{2}\right)}{\frac{k}{2}}\right)^4. \tag{26}$$

The truncation of the infinite summation in (25) is possible due to the exponential decay of the magnitude of $a(i)$'s for increasing values of i. Note that i represents the separation between $\phi_n, \phi_{n'}$.

Considering for the sake of simplicity that the electric field has been expanded in Battle–Lemarie scaling functions only (S-MRTD), based on (25), the discretized form of (9) according to this scheme is (instead of (13)):

$$_{k+1}E_m^\phi = {}_{k-1}E_m^\phi + \frac{c\Delta t}{\Delta z}\sum_{i=-n_a}^{i=n_a} a(i)\,_kE_{m+i}^\phi \tag{27}$$

It is evident in the latter expression, that due to the entire domain nature of the Battle–Lemarie basis, the stencil of the method extends over $2n_a + 1$ points. A choice of $n_a = 15$ brings about a truncation error that is absolutely less than 0.1%. In mathematical terms, S-MRTD approximates the spatial partial derivative $\partial/\partial z$ that appears on the right hand-side of the wave equation (9) by a thirty one point sum, while FDTD approximates the same expression by a second order accurate centered difference. In addition, the extended stencil of the method, and the non-localized character of the basis functions, calls for the use of the image principle for the modeling of localized, hard boundary conditions, such as perfect electric/magnetic conductors (Katehi *et al.* 1998).

Because of the high order (multi-point) approximation of spatial derivatives that they employ, Battle–Lemarie MRTD schemes have a highly linear dispersion behavior[3] (Krumpholz and Katehi 1996), that allows for the efficient modeling of electromagnetic structures at discretization rates that

---

[3] The effect of phase errors in the solution of a partial differential equation because of the discretization of the continuous interval on which it is defined is called numerical dispersion.

approach the Nyquist limit ($\lambda/2$). Therefore, an economy in memory of up to two orders of magnitude compared to the conventional FDTD is attainable by this method. Space adaptivity via thresholding of wavelet coefficients has been shown to further extend the computational efficiency of the method (Tentzeris *et al.* 1997), providing a straightforward implementation of adaptive subgridding.

On the other hand, high order approximations of spatial derivatives involved in Battle–Lemarie MRTD schemes, have as a negative consequence the decay of the stability factor of the latter, which becomes even more dramatic with the addition of wavelets. In particular, for a three dimensional S-MRTD scheme for the solution of Maxwell's curl equations in a uniform grid $\Delta x = \Delta y = \Delta z = \Delta$, the choice of the time step is limited by the condition (Krumpholz and Katehi 1996):

$$\Delta t \leq 0.368112 \frac{\Delta}{c} \tag{28}$$

while the respective condition for FDTD is (Taflove 1995):

$$\Delta t \leq 0.57735 \frac{\Delta}{c} \tag{29}$$

By adding only one level of wavelets, the condition in (28) becomes (Krumpholz and Katehi 1996):

$$\Delta t \leq 0.253064 \frac{\Delta}{c} \tag{30}$$

As an example, results from a three dimensional S-MRTD scheme applied to an air-filled, rectangular waveguide cavity of dimensions $1\,m \times 2\,m \times 1.5\,m$ are shown in Table 1 (Krumpholz and Katehi 1996; 1997). By inspection of these results, the conclusion that Battle–Lemarie MRTD allows the use of coarse grids (MRTD grid is in this case coarser by a factor of five per

Table 1. Resonant frequencies of an air-filled cavity with S-MRTD (Battle–Lemarie scaling functions only) and FDTD (Krumpholz and Katehi 1997)

Analytic values (MHz)	$2 \times 4 \times 3$ MRTD (MHz)	$10 \times 20 \times 15$ FDTD (MHz)
125.00	125.10	124.85
180.27	180.50	179.75
213.60	214.60	212.40
246.22	248.70	244.50
250.00	251.00	248.70
301.04	303.90	298.95
336.34	339.20	334.35

dimension compared to FDTD), yet maintaining an excellent accuracy, is deduced.

The generality of the moment method approach for deriving time domain schemes and the capability of the Battle–Lemarie basis to become a tool for memory efficient numerical modeling, have been demonstrated by the S-MRTD analysis of nonlinear pulse propagation (Krumpholz *et al.* 1997). In this work, the moment method is used to discretize a system of equations of the form:

$$
\frac{\partial E_F}{\partial z} + \frac{n_0}{c}\frac{\partial E_F}{\partial t} = j\kappa E_B \mathrm{e}^{-2j\Delta\beta z} + j\gamma\left(|E_F|^2 + 2|E_B|^2\right)E_F
$$
$$
\frac{\partial E_B}{\partial z} + \frac{n_0}{c}\frac{\partial E_B}{\partial t} = j\kappa E_F \mathrm{e}^{-2j\Delta\beta z} + j\gamma\left(|E_B|^2 + 2|E_F|^2\right)E_B. \tag{31}
$$

This set of equations, derived in (Winful 1985), describes the coupling between the forward and the backward fields, E_F, E_B under the slowly varying envelope approximation. Qualitatively, the cubic terms of the right hand side correspond to self-phase modulation, while the linear terms on the left hand side correspond to the dispersive coupling between the forward and the backward fields. FDTD and MRTD pulse modeling results and requirements are compared in Table 2. It becomes evident that even one tenth of the FDTD grid points is sufficient for MRTD to yield a reasonably accurate approximation of the peak of the transmitted pulse.

Moreover, the range of applications that have been demonstrated so far includes printed transmission line analysis (Tentzeris *et al.* 1996), nonlinear circuit modeling (Roselli *et al.* 1998), complex air-dielectric boundary problems and antenna geometries (Robertson *et al.* 1999). For the efficient simulation of open boundaries, a perfectly matched layer absorber for MRTD has been recently proposed (Tentzeris *et al.* 1999) and 8–16 cells are sufficient to obtain reflections limited to less than -80 dB.

3.3. HAAR MRTD SCHEMES

Due to their relative simplicity, Haar MRTD schemes present an attractive alternative to their entire domain counterparts and have therefore become

Table 2. Peak intensity of the transmitted pulse in a nonlinear medium via FDTD and MRTD (Krumpholz *et al.* 1997)

Grid points	FDTD	MRTD
100	–	10.407
200	7.969	10.623
500	10.189	–
1000	10.562	–

the subject of several studies in the recent literature (Goverdhanam *et al.* 1997; Fujii and Hoefer 1998; Goverdhanan and Katehi 1999). In addition, arbitrary order Haar MRTD schemes that provide the potential of performing dynamically adaptive simulations with arbitrary order mesh refinements have been presented (Sarris and Katehi 1999a, b). The formulation of the latter is based on the closed form evaluation of integrals of the same type as the ones in Equation (24).

A disadvantage of the Haar basis is that its spectral characteristics do not permit a very coarse gridding close to the Nyquist limit at the scaling function level. However, when a sufficiently dense scaling grid (of at least five points per wavelength) has been introduced and still a local mesh refinement is necessary for the modeling of some geometric detail, a Haar MRTD scheme with several orders of wavelets can be the method of choice.

As an example, the TEM propagation of a 0–20 GHz Gaussian pulse down a transmission line is simulated with a second order Haar wavelet scheme (of three wavelet levels). The parameters of the simulation are given in Table 3. The direction of propagation is the z-axis and the electric field has its only component parallel to the x-axis.

The scaling cell is chosen to be $\lambda_{min}/5$ and therefore, the resolution of this scheme is equal to fourty points per wavelength. In Fig. 7, the propagating pulse as modeled by this scheme is compared to the exact solution of the problem. An excellent correspondence of the MRTD solution to the exact solution can be observed. Despite the relatively coarse scaling grid, the MRTD solution is shown to be numerically dispersionless, preserving throughout its propagation the maximum value of the pulse. The absolute values of the individual scaling and wavelet contributions to the pulse at a certain time step are shown in Fig. 8. From this figure it also becomes evident that wavelet terms assume significant values at regions of high pulse derivatives. In addition, the higher the order of a wavelet term, the more concentrated around the derivative peak is the region where this term becomes significant.

Due to the latter property, significant economy in memory requirements of MRTD with respect to FDTD is expected. For the case study of the wave propagation that was earlier presented, this advantage is demonstrated in Fig. 9, where the number of MRTD coefficients for E_x after thresholding

Table 3. Parameters of the Haar wavelet simulation of TEM pulse propagation (Fig. 7)

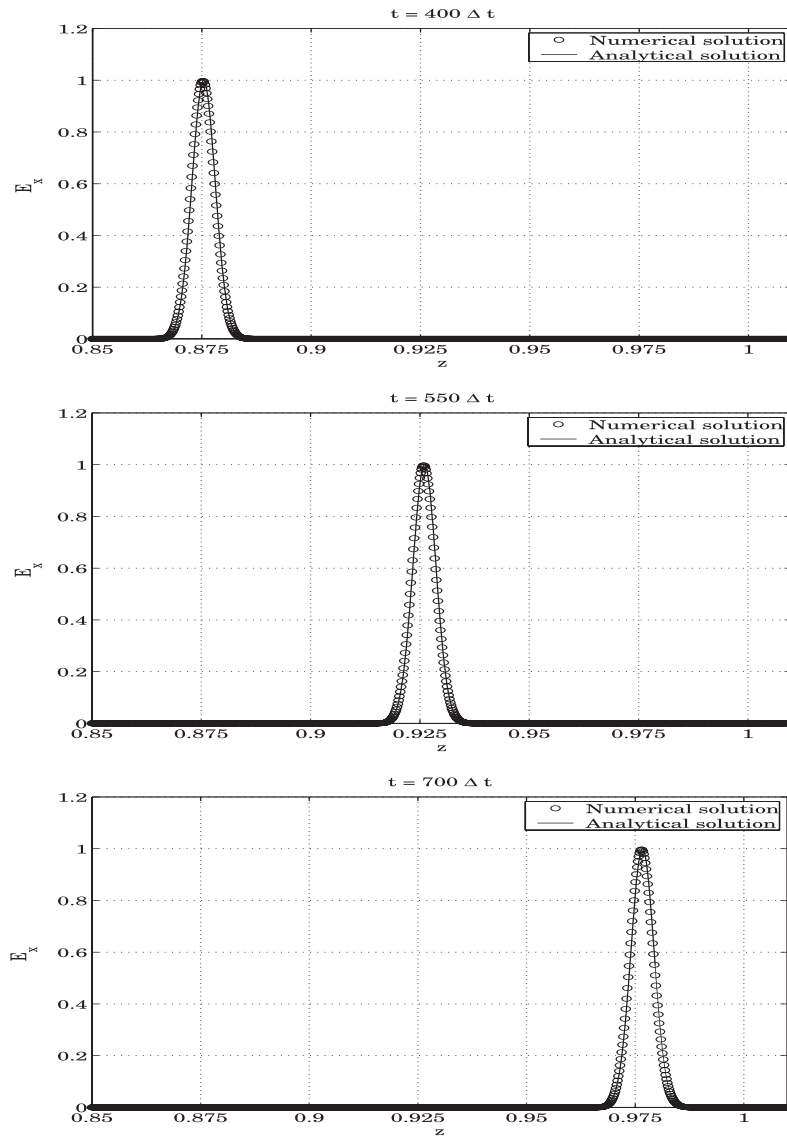| Parameter	Value
f_{max}	20 GHz
Time step, Δt	2.25 psec
Space step, Δz	1.5 mm
CFL number	0.9

Fig. 7. Haar wavelet modeling (2nd order scheme) of TEM pulse propagation.

with an absolute threshold of 10^{-6} is compared to FDTD coefficients for the same resolution, and their ratio (%) is plotted. It is observed that this ratio starts from $0.125 = 1/8$ as expected since at the beginning of the simulation all coefficients are zero and therefore only scaling terms remain after thresholding. As the pulse propagates along the transmission line, the ratio gradually increases, but still remains limited to less than 0.25. The thresholded and unthresholded waveforms are presented in the same figure, where
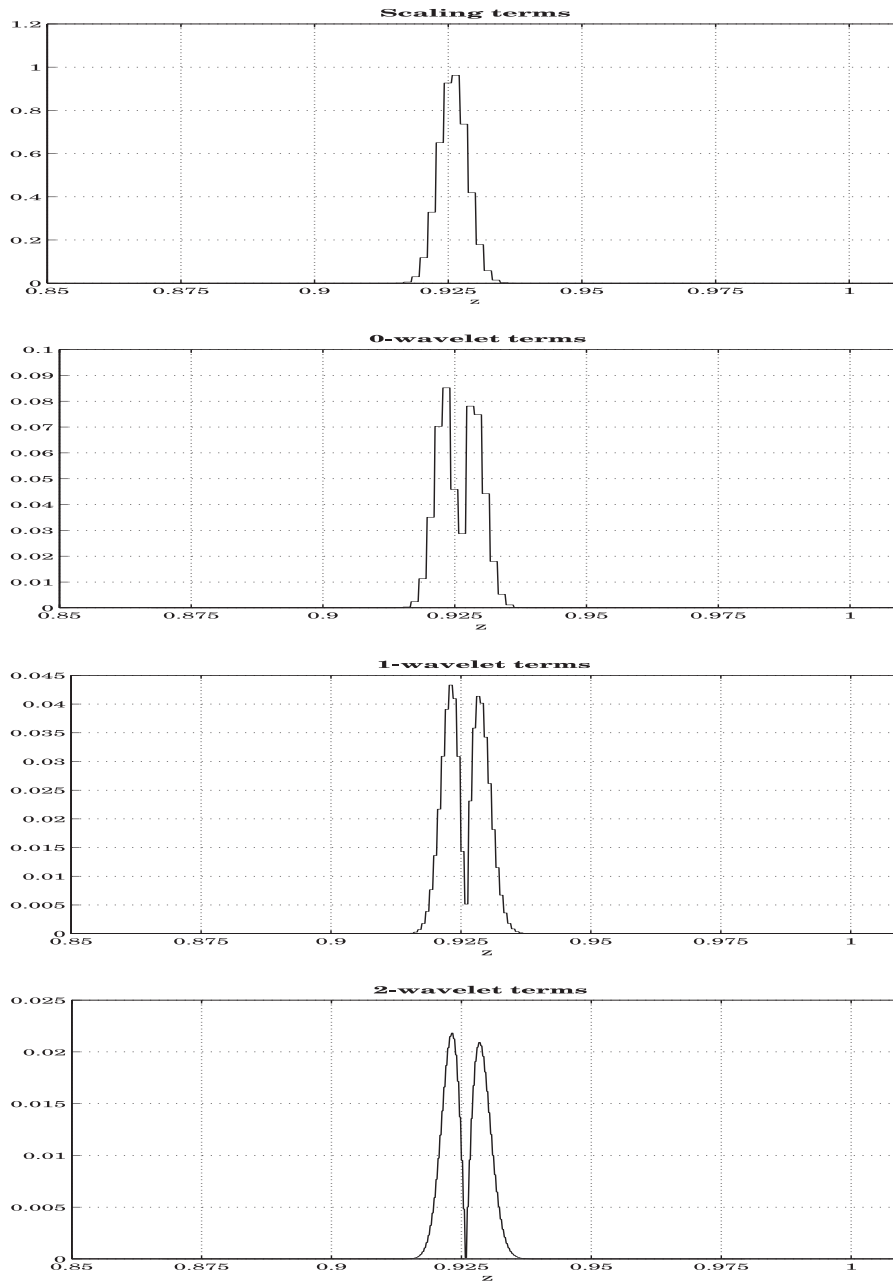
Fig. 8. Decomposition of the pulse (at $t = 550\,\Delta t$) into its multiresolution constituents.

excellent agreement between the two is observed. Hence, for the relatively low threshold of 10^{-6}, significant economy in memory has been achieved, while the accuracy of the solution has also been maintained.
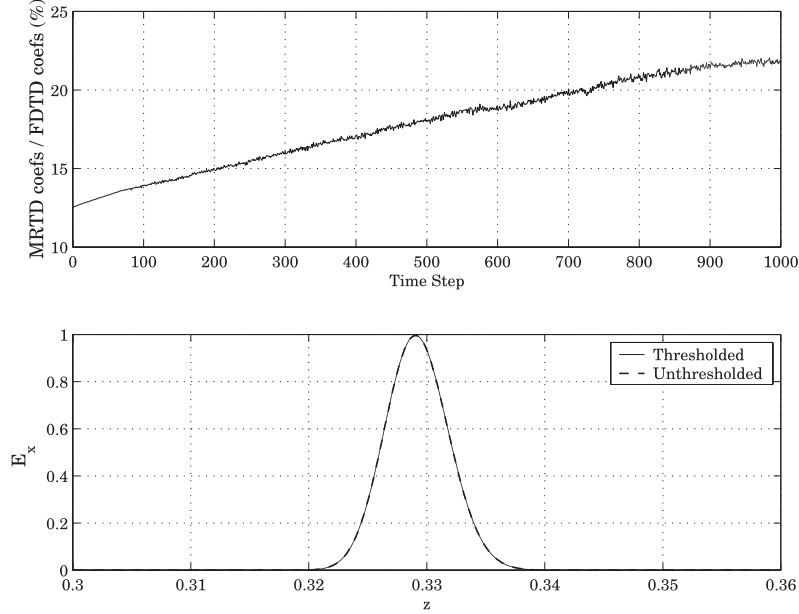
Fig. 9. Memory compression in Haar MRTD (2nd order) and comparison of thresholded and unthresholded waveforms, for a threshold of 10^{-6} at the time step $k = 1000\Delta t$.

A stability analysis of Haar MRTD shows that the minimum time step that renders the scheme stable is twice that of FDTD for the same resolution (equal number of degrees of freedom). In particular, for a three dimensional scheme, where wavelets of order R have been introduced in all three directions, and $\Delta x = \Delta y = \Delta z = \Delta$, the stability condition for the time step is:

$$\Delta t \leq 0.57735 \frac{\Delta}{2^R c} \tag{32}$$

For the FDTD scheme to achieve the same resolution, cell sizes: $\Delta x = \Delta y = \Delta z = \Delta / 2^{R+1}$ have to be defined, corresponding to a stability condition that reads:

$$\Delta t \leq 0.57735 \frac{\Delta}{2^{R+1} c} = 2 \times 0.57735 \frac{\Delta}{2^R c} \tag{33}$$

and limits the FDTD time step to half the MRTD time step at maximum.

4. Wavelet based frequency domain schemes

For the frequency domain analysis of electromagnetic geometries, the MoM has long been established as a tool for rigorous study. However, integral

based techniques combined with MoM, often lead to matrix equations that are difficult to be numerically solved due to their large number of unknowns and the non-sparse character of the matrix. Therefore, a major challenge for the successful application of MoM to problems of interest, is the choice of appropriate basis functions that render the matrix sparse, thus facilitating the numerical treatment of the related system of equations. A study of the representation of operators in wavelet bases has led to the conclusion, that the projections of integral operators onto wavelet bases usually correspond to highly sparse matrices (Beylkin *et al.* 1991). Since those matrices enjoy very good condition numbers, removing matrix elements of relatively small magnitude by a thresholding procedure does not result in significant degradation of the accuracy of the solution. Furthermore, this thresholding procedure amounts to removal of ill-conditioned elements from the moment matrix at the cost of losing some details (Sabetfakhri 1995). The construction of fast numerical algorithms is also assisted by an inherent property of the wavelet transform, according to which coefficients at a certain resolution can be recursively derived from coefficients at finer resolutions, by an iterative, filtering-like procedure (Mallat 1989). Hence, moment matrix elements at consecutive resolution levels can be recursively computed by the elements corresponding to the highest resolution. These concepts have been applied to a large number of guiding and radiating structures (Steinberg and Leviatan 1993; Sabetfakhri and Katehi 1995; Wang and Pan 1995). In these applications, taking full advantage of the wavelet transform properties has led to efficient numerical solvers combined with highly sparse moment matrices.

As an example, the two dimensional problem of electromagnetic field scattering from a slab waveguide of dielectric permittivity ϵ_r (Fig. 10) is considered. For the integral equation formulation of the problem, the
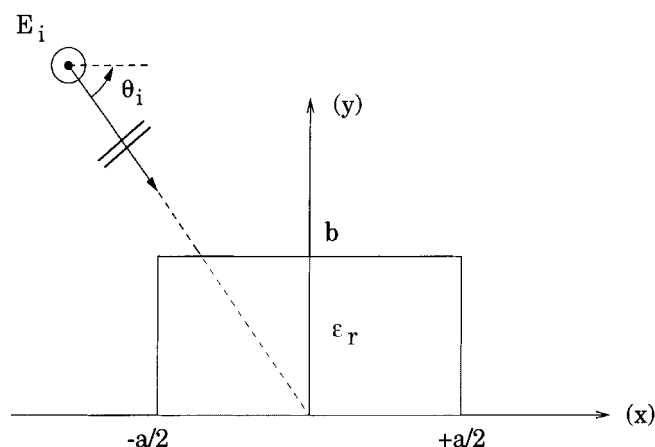

Fig. 10. Dielectric slab geometry.

dielectric region is replaced by a polarization current $\bar{J}_p$ extending over that region and given by the formula:

$$\bar{J}_p(x,y) = j\omega\epsilon_0(\epsilon_r - 1)\bar{E}(x,y) \quad |x| \le a/2, \quad 0 \le y \le b \tag{34}$$

Then, the electric dyadic Green's function of the problem (here corresponding to free space) is determined in the form (Yaghjian 1980):

$$\bar{\bar{G}}_e(x,y,x',y') = \bar{\bar{G}}_{oe}(x,y,x',y') + \hat{z}\hat{z}\frac{1}{k_0^2}\delta(x-x')\delta(y-y') \tag{35}$$

Also, the total electric field is divided into the (known) incident and the (unknown) scattered field:

$$\bar{E}(x,y) = \bar{E}_i(x,y) + \bar{E}_s(x,y) \tag{36}$$

Considering the scattered field as the response of the structure to the excitation of the polarization current $\bar{J}_p$ (that is induced by the interaction of the incident field with the dielectric slab), the electric field integral equation is written as (Chew 1990):

$$\bar{E}_s(x,y) = -j\omega\mu \iint_{\text{slab}} dx'dy'\bar{\bar{G}}_e(x,y,x',y') \cdot \bar{J}_p(x',y') \tag{37}$$

By a simple algebraic manipulation, the latter can be cast in the form:

$$\left(\frac{1}{\epsilon_{r-1}}\bar{\bar{I}} - \hat{z}\hat{z}\right) \cdot \bar{J}_p(x,y) - k_0^2 \iint_{\text{slab}} dx'dy' \,\bar{\bar{G}}_{oe} \cdot \bar{J}_p(x',y') = j\omega\epsilon_0\bar{E}_i(x,y) \tag{38}$$

Assuming that the incident field is vertically polarized,

$$\bar{E}_i(x,y) = \hat{z}E_0 e^{-j\bar{k}_i\cdot\bar{r}} = \hat{z}E_0 e^{-jk_0 x \cos\theta_i + jk_0 y \sin\theta_i} \tag{39}$$

both the scattered field and the polarization current are in the same direction. Hence, the unknown in (38) is the z-component of the polarization current, J_{pz}. Also, assuming that the slab is sufficiently thin in the y direction, J_{pz} can be considered as a function of x only (reduction to one dimension). For the solution of this problem, the MoM (Harrington 1968) combined with Multiresolution Analysis is applied. First, $J_{pz}(x)$ is expressed as a multiresolution expansion:

$$J_{pz}(x) = \sum_k c_k \phi\left(\frac{x}{\Delta x} - k\right) + \sum_j \sum_k d_{j,k}\psi\left(2^j \frac{x}{\Delta x} - k\right) \tag{40}$$

Similarly, the incident field is expanded as:

$$E_0 \mathrm{e}^{-jk_0 x \cos\theta_i} = \sum_k E_{i,k}^\phi \phi\left(\frac{x}{\Delta x} - k\right) + \sum_j \sum_k E_{i,k}^{\psi_j} \psi\left(2^j \frac{x}{\Delta x} - k\right) \tag{41}$$

The discretization rate Δx defines the resolution of the scaling function and presents an initial crude approximation of the solution that is refined by the wavelet levels. Substituting (40) and (41) into (38) and testing the resulting expression with the complex conjugate of the basis functions, results in a linear system of equations with respect to the unknown coefficients c_k, $d_{j,k}$, of the form:

$$\left[\begin{array}{c|c} A^{\phi\phi} & A^{\phi\psi} \\ \hline A^{\psi\phi} & A^{\psi\psi} \end{array}\right] \cdot \left[\begin{array}{c} \bar{c} \\ \bar{d} \end{array}\right] = \left[\begin{array}{c} \bar{E}_i^\phi \\ \bar{E}_i^\psi \end{array}\right] \tag{42}$$

where the multiresolution expansion coefficients $c_k, d_{j,k}, E_{i,k}^\phi, E_{i,k}^{\psi_j}$ have been incorporated into the vectors $\bar{c}, \bar{d}, \bar{E}_i^\phi, \bar{E}_i^\psi$ respectively.

While a well known bottleneck of this method is that for conventional bases, the matrix of the linear system (42) is densely populated and poorly conditioned, the use of wavelet bases renders this matrix sparse and significantly improves the condition number of the system. In the literature, matrix sparsities of even 99% have been reported (Sabetfakhri and Katehi 1996). In this example, the use of Haar basis leads to a matrix sparsity of 82.7% (originally the matrix had 65×65 elements), while a Battle–Lemarie basis leads to a higher matrix sparsity of around 95% (originally the matrix had 297×297 elements). In both cases, the moment matrices were rendered sparse by thresholding to zero all matrix elements whose magnitude was less than .01 of the maximum magnitude of all matrix entries. The structure of the moment matrix for each of the two case studies is shown in Figs. 11 and 12 respectively.

Finally, it is noted that the effect of the thresholding procedure on the accuracy of the solution is of the order of the threshold itself, mainly because of the good condition numbers that multiresolution moment matrices enjoy.

5. Conclusion

Several aspects regarding the application of wavelets to the numerical modeling of electromagnetic structures have been presented. It has been shown that the introduction of this relatively new theory to the field of electromagnetics has positively affected the existing time and frequency domain modeling techniques, improving their efficiency as well as their capa-
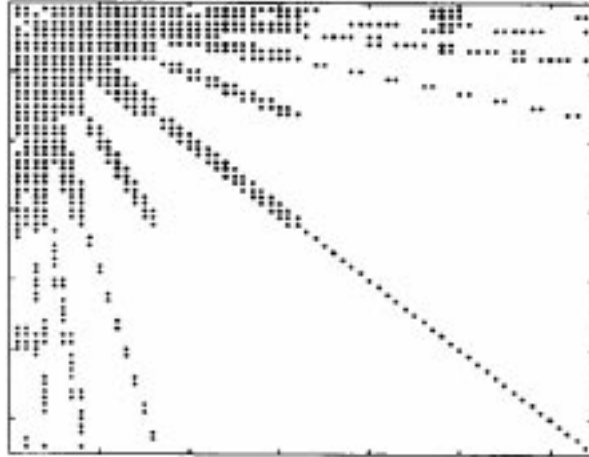
Fig. 11. Moment matrix structure for Haar wavelet MoM: A 1% threshold has given an 82.7% sparsity.
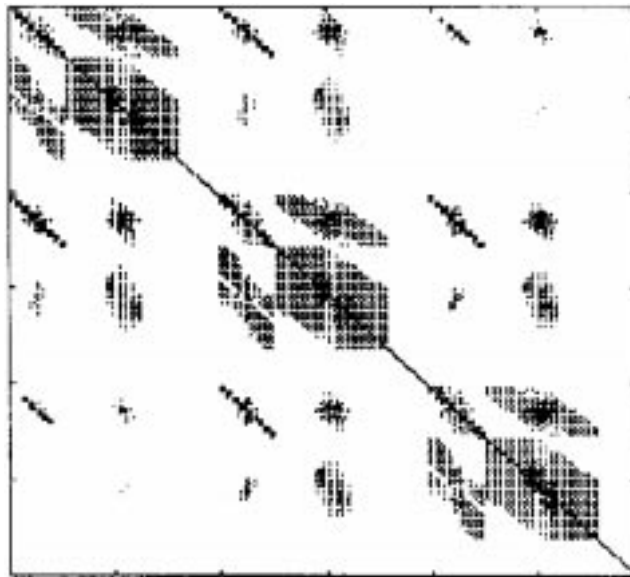

Fig. 12. Moment matrix structure for Battle–Lemarie wavelet MoM: A 1% threshold has given a 95% sparsity.

bility to treat large scale, complex problems. Although the scope of this study was to provide a general view of wavelet based techniques, it is hoped that it has also provided the necessary pointers that the interested reader may exploit to transfer the herein presented concepts to his/her own field of study.

Among the fields in which further application of wavelet based numerical analysis seems to be quite promising are circuit problems for CAD applications and nonlinear optics problems, in which the localized singular structure of the solution can be adaptively modeled by means of locally introduced wavelets.

Acknowledgement

References

Aidam M. and P. Russer. Application of Biorthogonal B-Spline-Wavelets to Telegrapher's Equations. In: *Proc. 14th Annual Review of Progress in Applied Computational Electromagnetics*, 983–990. Monterey, CA, 1998.

Bacry, E., S. Mallat and G. Papanicolaou. *Mathematical Modeling and Numerical Analysis* **26** 793, 1992.

Battle, G. *Comm. Math. Phys.* **110** 601, 1987.

Berger, M. and J. Oliger. *J. Comput. Phys.* **53** 484, 1984.

Beylkin, G., R. Coifman and V. Rokhlin. *Commun. Pure Appl. Math.* **44** 141, 1991.

Chew, W.C. *Waves and Fields in Inhomogeneous Media*, 378–381. Van Nostrand, 1990.

Cohen, A., I. Daubechies and J. Feauveau. *Comm. Pure Appl. Math.* **45** 485, 1992.

Daubechies, I. *Ten Lectures on Wavelets*, SIAM, Philadelphia, PA, 1992.

Fujii, M. and W.J.R. Hoefer. *IEEE Trans. Microwave Theory Tech.* **46** 2463, 1998.

Goverdhanam, K., C.D. Sarris, M.M. Tentzeris and L.P.B. Katehi. A PML Absorber Formulation for Haar Wavelet Based MRTD, In: *Proc. of the 1999 European Microwave Conference,* Munich, Germany

Goverdhanam, K., L.P.B. Katehi and A.C. Cangellaris, *Proc. IEEE Int. Sym. on Microwave Theory Tech.* 333–336, 1997.

Goverdhanam K. and L.P.B. Katehi. *Proc. IEEE Sym. on Microwave Theory Tech.* 1999.

Haar, A. *Math. Ann.* **69** 331, 1910.

Harrington, R.F. *Field Computation by Moment Methods*, Macmillan, New York, 1968.

Katehi, L.P.B., J.F. Harvey and E.M. Tentzeris. *Time Domain Analysis Using Multiresolution Expansions, Chapter in Advances in Computational Electromagnetics: The Finite Difference Time Domain Method*, Artech House, Norwood, MA, 1998.

Krumpholz, M. and L.P.B. Katehi. *IEEE Trans. on Microwave Theory Tech.* **44** 555, 1996.

Krumpholz, M. and L.P.B. Katehi. *Proc. IEEE Microwave Symposium Workshop on Wavelets in Electromagnetics*, 1997.

Krumpholz, M., C. Huber and P. Russer. *IEEE Trans. on Microwave Theory Tech.* **43** 1935, 1995.

Krumpholz, M., H.G. Winful and L.P.B. Katehi. *IEEE Trans. Microwave Theory Tech.* **45** 385, 1997.

Mallat, S. *A Wavelet Tour of Signal Processing*, Academic Press, 1998.

Mallat, S. *IEEE Trans. Pattern Anal. Machine Intell.* **PAMI-7** 674, 1989.

Meyer, Y. *Wavelets and Operators*, Cambridge University Press, 1992.

Robertson, R.L., E.M. Tentzeris and L.P.B. Katehi. *Proc. IEEE Int. Sym. on Microwave Theory Tech.* 1999.

Roselli, L., E.M. Tentzeris and L.P.B. Katehi. Nonlinear Circuit Characterization Using a Multiresolution Time Domain Technique. In: *Proc. of the 1998 MTT-S Conference*, 1387–390, Baltimore, MD, 1998.

Sabetfakhri, K. *Novel Efficient Integral-based Techniques for Characterization of Planar Microwave Structures*, Ph.D. diss., University of Michigan, 1995.

Sabetfakhri, K. and L.P.B. Katehi. On the Application of Quasi-Wavelet Expansion to Open Dielectric Waveguide Problems. In: *Proc. IEEE Antennas Prop. Symp*. Ann Arbor, 1993.

Sabetfakhri, K.F. and L.P.B. Katehi. *IEEE Microwave Guided Wave Lett*. **6** 19, 1996.

Sarris, C.D. and L.P.B. Katehi. *Proc. IEEE Int. Sym. on Microwave Theory Tech.* 1999.

Sarris, C.D. and L.P.B. Katehi. Formulation and Study of an Arbitrary Order Haar Wavelet Based Multiresolution Time Domain Technique. In: *16th Annual Review of Progress in Applied Computational Electromagnetics Conference*, Monterey, CA, 2000.

Steinberg, B.Z. and Y. Leviatan. *IEEE Trans. Antennas Prop*. **41** 610, 1993.

Strikwerda, J.C. *Finite Difference Schemes and Partial Differential Equations*. Wadsworth Inc., Belmont, CA, 1989.

Taflove, A. *Computational Electrodynamics: The Finite Difference Time Domain Method*, Artech House, Norwood, MA, 1995.

Tentzeris, E.M., M. Krumpholz and L.P.B. Katehi. In: *Proc. IEEE Int. Sym. on Microwave Theory Tech.* 573, 1996.

Tentzeris, E.M., R.L. Robertson, A.C. Cangellaris and L.P.B. Katehi. *Proc. IEEE Int. Sym. on Microwave Theory Tech.* 337, 1997.

Tentzeris, E.M., R.L. Robertson, J.F. Harvey and L.P.B. Katehi. *PML absorbing boundary conditions for the characterization of open microwave circuit components using multiresolution time domain techniques (MRTD)*, to appear in the IEEE Trans. Antennas and Prop.

Wang, G. and G.W. Pan. *IEEE Trans. Microwave Theory Tech*. **43** 131, 1995.

Winful, H.G. *Appl. Phys. Letters* **46**(6), 527, 1985.

Yaghjian, A.D. *Proc. IEEE,* **68** 248, 1980.